Environ. Sci. Technol. **2004**, *38,* 3941−3949

Thermodynamic Properties of Multifunctional Oxygenates in Atmospheric Aerosols from Quantum Mechanics and Molecular Dynamics: Dicarboxylic Acids

CHINGHANG TONG, MARIO BLANCO, WILLIAM A. GODDARD III,* AND JOHN H. SEINFELD*

Departments of Environmental Science and Engineering, Chemical Engineering, and the Material and Process Simulation Center, California Institute of Technology, Pasadena, California 91125

Ambient particulate matter contains polar multifunctional oxygenates that partition between the vapor and aerosol phases. Vapor pressure predictions are required to determine the gas−particle partitioning of such organic compounds. We present here a method based on atomistic simulations combined with the Clausius−Clapeyron equation to predict the liquid vapor pressure, enthalpies of vaporization, and heats of sublimation of atmospheric organic compounds. The resulting temperature-dependent vapor pressure equation is a function of the heat of vaporization at the normal boiling point [$\Delta H_{vap}(T_b)$], normal boiling point (T_b), and the change in heat capacity (liquid to gas) of the compound upon phase change [$\Delta C_p(T_b)$]. We show that heats of vaporization can be estimated from calculated cohesive energy densities (CED) of the pure compound obtained from multiple sampling molecular dynamics. The simulation method (CED) uses a generic force field (Dreiding) and molecular models with atomic charges determined from quantum mechanics. The heats of vaporization of five dicarboxylic acids [malonic (C_3), succinic (C_4), glutaric (C_5), adipic (C_6), and pimelic (C_7)] are calculated at 500 K. Results are in agreement with experimental values with an averaged error of about 4%. The corresponding heats of sublimation at 298 K are also predicted using molecular simulations. Vapor pressures of the five dicarboxylic acids are also predicted using the derived Clausius−Clapeyron equation. Predicted liquid vapor pressures agree well with available literature data with an averaged error of 29%, while the predicted solid vapor pressures at ambient temperature differ considerably from a recent study by Bilde et al. (*Environ. Sci. Technol.* **2003**, *37*, 1371−1378) (an average of 70%). The difference is attributed to the linear dependence assumption that we used in the derived Clausius−Clapeyron equation.

Introduction

Atmospheric gas−particle partitioning of organic compounds is governed strongly by the vapor pressure of the compound (subcooled if necessary) as well as its liquid-phase activity coefficient (*1*−*4*). However, data are not available for the subcooled vapor pressures as a function of temperature for many organic compounds in atmospheric aerosols. These subcooled liquid vapor pressures for compounds that are solid at the temperature of interest are usually determined only indirectly by experiments, and many methods used to estimate vapor pressure (*5*, *6*) are typically from correlations with other data. Consequently, reliable and fast theoretical estimation techniques would be most useful. We propose an alternative that makes use of the advances in computational and theoretical chemistry to calculate the parameters needed to predict the thermodynamic properties of interest.

Dicarboxylic acids [$HOOC(CH_2)_{n-2}COOH$] are of particular importance as ubiquitous components of atmospheric aerosols (*7*−*12*). They generally have low vapor pressures and, therefore, are expected to partition to the condensed phase. The gas−particle partitioning of these acids, and indeed of all organic atmospheric compounds, depends critically on the values of their vapor pressures. Their melting temperatures are in the range of 372−461 K, and their boiling temperatures are within the range of 573−623 K (Table 1) (*13*, *14*, *16*). As a result, the relevant vapor pressures for determination of gas−particle partitioning of the dicarboxylic acid at ambient temperature are the subcooled liquid vapor pressures.

Limited experimental solid vapor pressure data are available for the dicarboxylic acids at ambient temperature. Recently, Bilde et al. (*18*) inferred vapor pressures and heats of sublimation for C_3−C_9 dicarboxylic acids from measured evaporation rates at ambient temperature using the tandem differential mobility analyzer (TDMA) technique.

The vapor pressures of glutaric acid and adipic acid have also been determined by Tao and McMurry (*19*) using TDMA. Chattopadhyay et al. (*20*) measured the vapor pressures of C_6−C_8 dicarboxylic acids using temperature-programmed thermal desorption. At higher temperatures, vapor pressure data were reported by Davies and Thomas (*21*) for C_4−C_{16} even carbon-numbered dicarboxylic acids and by Ribeiro da Silva et al. (*22*) for C_3−C_{11} odd carbon-numbered acids using the effusion method.

An intriguing feature of the thermodynamic properties of the unsubstituted dicarboxylic acids is that the vapor pressures and the heats of sublimation both alternate strongly with the parity of the number of carbon atoms. Such odd and even alternation is a result of the difference in the solid-state structures between odd and even acids. Thalladi et al. (*23*) found that, in the solid, the odd acid molecules pack to form twisted conformations, whereas the even acids have planar molecular conformations. Bilde et al. (*18*) suggested that the alternation in vapor pressures and heats of sublimation could be attributed to this torsional strain in the odd carbon-numbered acids.

In this paper, we present a method based on atomistic simulations for predicting the liquid vapor pressure of organic compounds. The method is applied to predict the vapor pressures of malonic (C_3), succinic (C_4), glutaric (C_5), adipic (C_6), and pimelic (C_7) acids. In addition to dicarboxylic acids, we have also applied the method to formic, acetic, and benzoic acids. Predicted vapor pressures are compared to those measured experimentally. Finally, an assessment of the main uncertainties in the theoretical method is given.

Vapor Pressure Estimation Method

The vapor pressure of an organic compound can be obtained by integrating the total enthalpy of vaporization over

* Address correspondence to either author. Phone: (626)395-2730; fax: (626)585-0918; e-mail: wag@wag.caltech.edu (W.A.G.). Phone: (626)395-4635; fax: (626)796-2591; e-mail: seinfeld@caltech.edu (J.H.S.).

10.1021/es0354216 CCC: $27.50
Published on Web 06/11/2004

TABLE 1. Experimental Physical Properties of C_3−C_7 Dicarboxylic Acids

	malonic	succinic	glutaric	adipic	pimelic
no. of carbons, *n*	3	4	5	6	7
MW (g/mol)	104.1	118.1	132.1	146.1	160.2
melting point, T_m (K)[a]	408 ± 0.3	461 ± 0.3	371 ± 0.9	426 ± 0.3	378 ± 0.4
boiling point, T_b (K)[b]	580	591	576.15	610.65	615.25
density (g/cm^3)[c]	1.616	1.566	1.414	1.362	1.281
entropy of fusion at T_m, $\Delta S_{fus}(T_m)$ (J/mol)	62.28	71.43	61.80	81.90	80.34

[a] Values of melting point and their uncertainties are obtained from the NIST Chemistry Webbook (*14*). [b] Boiling points C_3−C_4 diacids (*15*) are obtained from DIPPR tables (*13*). Values for C_5−C_6 diacids are obtained from the CRC Handbook (*16*). Uncertainties are estimated to be 10% for C_3−C_6 diacids. Boiling point of the C_7 acid is from Stull's study, and the uncertainty is 5% (*17*). [c] Densities at 298 K from ref 23.

TABLE 2. Averaged Values of CED and Density for Dicarboxylic Acids and Their Calculated Heats of Vaporization at 500 K

	malonic	succinic	glutaric	adipic	pimelic
no. of carbons, *n*	3	4	5	6	7
target density (g/cm^3) at 500 K	1.2863	1.1642	1.0909	1.0228	1.0759
simulation density (g/cm^3) at 500 K	1.27 ± 0.04	1.14 ± 0.04	1.06 ± 0.05	1.01 ± 0.05	0.97 ± 0.04
% difference in density	−1.27	−2.08	−2.83	−1.25	−9.84
CED (J/cm^3) at 500 K	1010.56 ± 56.90	821.57 ± 51.92	686.30 ± 60.71	623.29 ± 40.46	563.54 ± 46.69
literature ΔH_{vap}(500 K) (kJ/mol)	81.47	83.87	84.46	83.84	89.97
calcd ΔH_{vap}(500 K) without ZPE correction (kJ/mol)	86.96 ± 5.61	89.26 ± 6.45	89.70 ± 8.99	94.34 ± 7.70	97.21 ± 9.00
Δ%[a]	6.74	6.43	6.19	12.53	8.05
calcd ΔH_{vap}(500 K) with ZPE correction (kJ/mol)	75.71 ± 4.88	82.48 ± 5.96	84.07 ± 8.43	87.47 ± 7.14	95.05 ± 8.80
Δ%	−7.08	−1.65	−0.47	4.33	5.65

[a] Δ% is the percentage deviation of the predicted value from the literature value.

temperature using the Clausius−Clapeyron equation (*24*, *25*), assuming that $\Delta H_{vap}(T)$ has a linear temperature dependence:

$$\Delta H_{vap}(T) = \Delta H_{vap}(T_b) + \Delta C_p(T_b)(T - T_b) \quad (1)$$

The resulting temperature-dependent equation for vapor pressure is a function of heat of vaporization at normal boiling point [$\Delta H_{vap}(T_b)$], the change in heat capacity of the compound upon phase change (ΔC_p), and the normal boiling point (T_b):

$$\ln P_L^s = -\frac{\Delta H_{vap}(T_b)}{R}\left(\frac{1}{T} - \frac{1}{T_b}\right) + \frac{\Delta C_p(T_b)}{R}\left(\frac{T_b}{T} - 1\right) - \frac{\Delta C_p(T_b)}{R}\ln\left(\frac{T_b}{T}\right) \quad (2)$$

Since the temperature dependence of the vapor pressure for the subcooled liquid is expected to follow the same dependence as that of the liquid state, eq 1 should be appropriate for estimating the subcooled vapor pressure (*25*). Equation 2 should reproduce both the magnitude and temperature dependence of the liquid vapor pressure.

Prediction of the Heats of Vaporization Using CED. The heat of vaporization at the normal boiling point, $\Delta H_{vap}(T_b)$, can be estimated from the cohesive energy density (CED). The CED of a pure liquid substance is defined as

$$\text{CED} = \frac{\Delta H_{vap}(T) - RT}{V_m} \quad (3)$$

where V_m is the molar volume.

The CED of a pure compound can be calculated using multiple sampling molecular dynamics (MD) with periodic boundary conditions (*26*). The periodic unit cell for these MD simulations is built with molecules having the appropriate conformation and atomic charges. We determine the atomic charges and geometries of the molecules using quantum mechanics (QM), with the B3LYP flavor of density functional theory (DFT) (*27*). Many studies show that DFT/B3LYP leads to reliable binding energies of hydrogen-bonded systems [e.g., water dimer (*28*) and dimers of DNA base (*29*)], suggesting that it should be accurate for describing the interaction between dicarboxylic acids. Given the appropriate geometry and atomic charges of the molecule from QM, the CED calculation proceeds as follows (*26*):

(i) A periodic unit cell containing 32 molecules is built at 50% of the target density ($0.5\rho_0$). The force field parameters are taken from the Dreiding force field (*30*) with the hydrogen-bonding parameters ($r_0 = 2.5$ Å, $D_0 = 7.5$ kcal/mol) modified to fit the QM results for the dimer using acetic acid dimer (see Appendix A). The building process constructs a disordered cell by inserting the molecules with random positions, orientations, and torsions and excludes cases with contact distances less than 30% of the equilibrium value. Ten such periodic cells are constructed, each independent of the other.

(ii) For each cell, we carry out a series of MD calculations as follows: (a) at $0.5\rho_0$ we minimize (MM) the structure [2000 steps or to an root-mean-square (RMS) force converging to 0.1 kcal/mol Å]. This is followed by 700 steps of MD (1 fs/steps) at 700 K using canonical fixed volume dynamics (NVT) to anneal the sample. (b) The cell coordinates are shrunk such that the density is increased to $0.675\rho_0$, and then the MM and MD steps are repeated holding the cell fixed. (c) A total of four compressions, minimization, dynamics (at densities of $0.675\rho_0$, $0.85\rho_0$, $1.025\rho_0$, and $1.2\rho_0$) are performed until the density reaches 120% of the target density (ρ_0) (d) This is followed by a total of four expansion, minimization, dynamics until the target density is reached (i.e., the same MM and MD steps at densities of $1.15\rho_0$, $1.10\rho_0$, $1.05\rho_0$, and ρ_0). The final density (ρ) of the cell is reported. (e) After that, the system with a density of ρ is energy minimized in 2000 steps allowing the cell parameters and atom coordinates to relax (to an RMS force of 0.1 kcal/mol and an RMS stress of 0.1 GPa).

(iii) Finally, a full 10 ps of NPT MD simulation is performed, allowing the cell and atom positions to optimize at the target temperature. The first half of the MD is used to thermalize

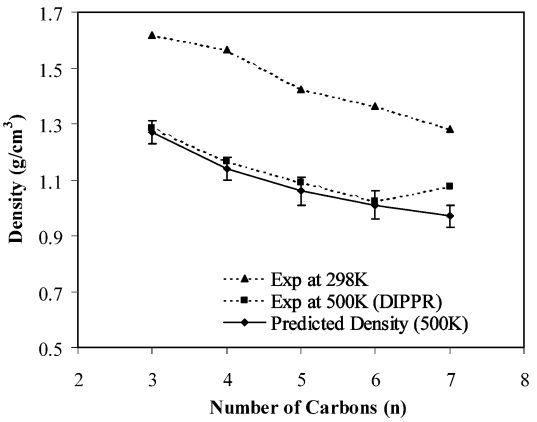

FIGURE 1. Comparison between predicted and initial target densities (experimental at 500 K) of the simulations. The experimental densities at 298 K are also shown.

the sample at the target temperature, and the second half of the MD is used to obtain the average cell volume and potential energies. The CED are calculated by subtracting the potential energy of the bulk system from the sum of the potential energies of the individual molecules as if separated by an infinite distance.

(iv) This procedure is repeated for all 10 independent cells from which the average CED and the standard deviation are computed. Sampling error follows statistical distribution for an average of N samples, i.e., $1/\sqrt{N}$.

The target temperature of the CED simulations was set at 500 K. At this temperature, all the selected dicarboxylic acids ($n = 3-7$) are in the liquid state, for which the liquid densities are available (*13*). With the CED simulation results, the heat of vaporization [$\Delta H_{vap}(T)$] of a compound is first computed at the target temperature using eq 3, and the molar volume (V_m) is calculated using the simulation density (ρ). The heat of vaporization at the normal boiling point [$\Delta H_{vap}(T_b)$] is then calculated using eq 1. We then estimate $\Delta S_{vap}(T_b) = \Delta H_{vap}(T_b)/T_b$, where the normal boiling points (T_b) are obtained from the literature (*13*, *14*, *16*).

We incur relatively little error by relating the $\Delta C_p(T_b)$ term to $\Delta S_{vap}(T_b)$. Over a series of compounds, it has been found that $\Delta C_p(T_b)/\Delta S_{vap}(T_b) = -0.8$ (*25*), thus for $\Delta C_p(T_b)$ we assume:

$$\Delta C_p(T_b) = -0.8\Delta S_{vap}(T_b) \quad (4)$$

Results and Discussion

Table 2 displays the results and the standard deviations of the CED and simulation density for the C_3-C_7 dicarboxylic acids [$HOOC(CH_2)_{n-2}COOH$, $n = 3-7$]. The DIPPR database contains values obtained from correlation between experimental results, which we refer to as "literature" values (*13*). Figures 1 and 2 compare the predicted and literature values for the heat of vaporization for C_3-C_7 dicarboxylic acids at 500 K; the target density and the final density of the simulation are also shown.

With the exception of pimelic acid, the final density from the simulations is 1.2−2.8% low at our target density of 500 K, indicating that the model provides a reasonable representation of the real system. The exception is pimelic acid where the DIPPR Database (*13*) gives a value 9.84% higher than our value. As indicated in Figure 1, the density of the C_7 diacid given by DIPPR Database (*13*) is well outside the trends in experimental values at 500 K. Experimental densities at 298 K (*23*) were also shown to illustrate such trends for C_3-C_7 diacids.

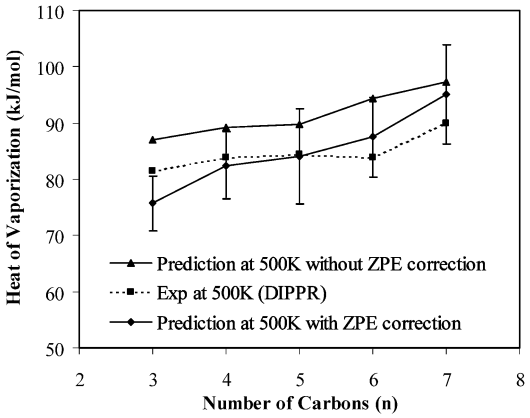

FIGURE 2. Predicted and experimental values of ΔH_{vap}(500 K).

The calculated heats of vaporization at 500 K are systematically high by 5.2−5.7 kJ/mol for $n = 3-5$, but high by 10.5 kJ/mol for $n = 6$ and 7.2 kJ/mol for $n = 7$ (Figure 2). These values are expected to be too high because we have not corrected for zero-point energy (ZPE). Because we freeze out the molecular geometries to estimate the average enthalpies of the gas-phase individual molecules, the intramolecular contributions should cancel out from ΔH_{vap}, but the intermolecular terms do not. The intermolecular ZPE for the crystalline forms range from −2.2 kJ/mol to −11.3 kJ/mol as shown in Table 3.

After the ZPE correction, the predictions are now low by 5.8 kJ/mol for $n = 3$, 1.4 kJ/mol for $n = 4$, and only 0.4 kJ/mol for $n = 5$. The predictions for $n = 6-7$ are still high, but the absolute errors are reduced to 3.6 kJ/mol for $n = 6$ and 5.1 kJ/mol for $n = 7$. All the predictions and their respective errors are shown in Table 2.

The parameters $\Delta H_{vap}(T_b)$ and $\Delta C_p(T_b)$ are then calculated using eqs 1−4, with molar volumes (V_m) calculated using the simulation densities. With these parameters (Table 4), the liquid vapor pressures for C_3-C_7 dicarboxylic acids are predicted using eq 2.

Measurements of the vapor pressures are available for these five acids over the temperature range of ~400 to ~600 K (*13*). The predicted liquid vapor pressures are compared with the experimental values in Figure 3, and our predictions differ from the experimental values on average by 29%.

At ambient temperature, solid vapor pressures of low molecular weight carboxylic acids have been measured using various methods (*18*−*20*). Most of these studies derive vapor pressures of the compounds from measurements of evaporation rates, and the heats of vaporization (sublimation for solids) were also calculated by assuming a Clausius−Clapeyron relationship (*18*−*22*). We also predicted heats of sublimation for the C_3-C_7 dicarboxylic acids using MD simulations, which are compared with available literature data (*18*−*22*) in Table 5. All values were determined at 298 K, with the exception of those given by Bilde et al. (*18*), which were calculated at 296 K (we assume that the 2 K temperature difference can be neglected).

Figure 4 shows the heats of sublimation of the dicarboxylic acids against number of carbons (n). While the calculated heats of sublimation for C_3-C_7 dicarboxylic acids agree reasonably with those of Riberio da Silva et al. (*22*), with an average of 3% difference and a maximum difference of ~7%, the predictions differ considerably from those of Bilde et al. (*18*) with an average error of 17%. In general, our predictions for even acids are better than those for odd acids. The predicted value for pimelic acid agrees well with two data sets with the exception of Chattopadhyay et al. (*20*).

Since experimental subcooled vapor pressures are not available in the literature, solid vapor pressures were

TABLE 3. Calculated Intermolecular Zero-Point Energy (ZPE) for C_3-C_7 Dicarboxylic Acid Crystals

	malonic	succinic	glutaric	adipic	pimelic
no. of carbons, *n*	3	4	5	6	7
ZPE for single molecule (kJ/mol)	201.64	279.29	359.23	437.61	516.65
no. of molecules in crystals	2	2	4	2	4
ZPE for crystals (kJ/mol)[a]	425.79	572.14	1459.43	888.98	2075.25
normalized intermolecular ZPE (kJ/mol)	−11.25	−6.78	−5.63	−6.88	−2.16

[a] The zero-point energy of the unit cells were calculated in the Brillouin zone (3,3,3).

TABLE 4. Input Parameters for C_3-C_7 Dicarboxylic Acids[a]

	malonic	succinic	glutaric	adipic	pimelic
no. of carbons, *n*	3	4	5	6	7
T_b (K)	580	591	576.15	610.65	615.25
V_m (cm³/mol)	81.94	103.59	124.64	144.70	165.12
$\Delta H_{vap}(T_b)$ (kJ/mol)	68.18 ± 6.11	73.43 ± 6.91	76.03 ± 8.99	76.39 ± 7.62	82.66 ± 8.97
$\Delta S_{vap}(T_b)$ (J/mol)	117.56	124.25	131.96	125.10	134.36
$\Delta C_p(T_b)$ (J/mol K)	−94.05	−99.40	−105.57	−99.99	−107.48

[a] These values are used in eq 2 to predicted liquid vapor pressures, and they are also used for uncertainties estimation. All of the values are calculated from the simulation results, with the exception of T_b, which was taken from the literature (*13*, *14*, *16*).

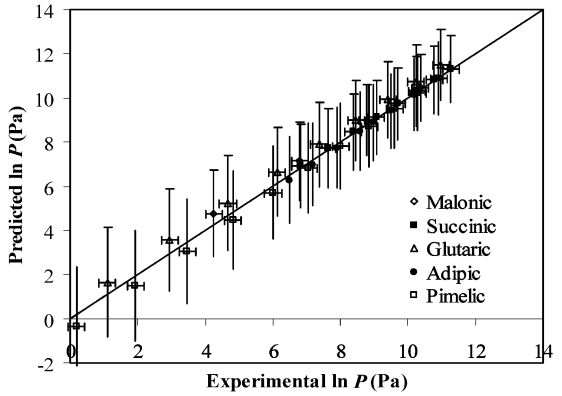

FIGURE 3. Comparison of predicted vs literature liquid vapor pressure, ln *P* (in units of Pa), over the temperature range of ~400 to ~600 K for C_3-C_7 dicarboxylic acids. The solid line is the 1:1 correspondence line. The average error over all points is 29%. Original references for malonic, succinic (*31*), glutaric (*32*), adipic (*17*), and pimelic (*31*) acids.

calculated from the predicted results using (*25*)

$$\ln P_S^s = \ln P_L^s - \frac{\Delta S_{fus}(T_m)}{R}\left(\frac{T_m}{T} - 1\right) \qquad (5)$$

Entropies of fusion at the melting point [$\Delta S_{fus}(T_m)$] and melting points (T_m) for C_3-C_7 dicarboxylic acids were obtained from the literature (*13, 14*) (Table 1). Calculated solid vapor pressures are compared with literature values in Figure 5.

It shows that the predictions for solid vapor pressure are relatively better (~21% error) at higher temperature (350−400 K), compared to the large discrepancy (~70% error) with Bilde et al. (*18*) at the lower temperature (~300 K). The discrepancy may be the result of our assumption that $\Delta H_{vap}(T)$ has a linear temperature dependence. A linear fit for the solid vapor pressure data in Figure 4 provides a correction factor equal to 0.844 with $R^2 = 0.979$, that is, experimental ln P_s = 0.844 (predicted ln P_s).

Figure 6a,b shows the predicted solid vapor pressures versus literature values at 298 and 365 K, respectively. At both temperatures, we capture qualitatively the odd−even alternation in vapor pressures. Our predictions at 365 K have an averaged error of 9.5% with the literature values, while the predictions of solid vapor pressure at 298 K have a larger averaged error of 71.5%. Overall, the predictions are considered satisfactory given the simplicity of the method and the substantial uncertainty involved in the low-pressure data.

We have shown that the new hydrogen-bonding parameters are appropriate for dicarboxylic acids. Since the new hydrogen-bonding parameters for carboxylic acid functional groups were determined using the formic and acetic acid dimer results, they should also be applicable to monocarboxylic acids. In addition to mono- and dicarboxylic acids, we have also examined the applicability of the new parameters to aromatic monocarboxylic acids (e.g., benzoic acids). The simulation results, normal boiling points, calculated $\Delta H_{vap}(T_b)$, and $\Delta C_p(T_b)$ for formic, acetic, and benzoic acids are shown in Table 6.

Liquid vapor pressures are calculated using eq 2, and the results were compared with available experimental data (*13*) (Table 7). The averaged error for formic acid is only 7.7% and 14.3% for acetic acids (Table 7 and Figure 7). For benzoic acid, we have a relatively larger discrepancy, corresponding to an averaged error of 31.2%. Nevertheless, it is still comparable with our averaged error for C_3-C_7 dicarboxylic acids (~29%).

We are relying on eq 1 to estimate heat of vaporization at temperatures other than $T = T_b$. Table 7 shows that vapor pressures are often underestimated below T_b for formic, acetic, and benzoic acids. Note that the error diminishes as we approach the boiling point. Thus, the approximation in eq 1 could be explained by a ΔC_p value that is overestimated by eq 4. In principle, we could adjust the value −0.8 in eq 4 to avoid such systematic underestimation of vapor pressures. However, from Figure 3, we notice that for glutaric acid we overestimate the vapor pressures. Therefore, we choose to keep eq 4 as in ref *25*.

Estimation of Uncertainties

Uncertainties of individual data points are shown in Figures 3, 5, and 7. According to the DIPPR database (*13*), the maximum error in the experimental liquid vapor pressure data is 25%. An error of 5% can be found in the normal boiling point data for pimelic (C_7) acid. Uncertainties for C_5 and C_6 diacids are not clearly given in the CRC Handbook (*16*). The normal boiling points for C_3 and C_4 diacids were obtained by the Lydersen method using the critical temperatures predicted by Thodos and Forman (*15*). Since most of the normal boiling point estimation methods incur errors ranging

TABLE 5. Predicted and Experimental Heats of Sublimation (kJ/mol) for C_3-C_7 Dicarboxylic Acids

	malonic	succinic	glutaric	adipic	pimelic
prediction	103.72 ± 5.70	114.37 ± 2.38	121.98 ± 2.57	132.55 ± 1.66	139.33 ± 2.07
exp. Ribeiro et al. (*22*)	111.4 ± 0.7	121.8 ± 3.3	119.8 ± 1.2	133.6 ± 1.3	139.9 ± 1.0
Δ%[a]	−6.9	−6.1	1.8	−0.8	−0.4
exp. Bilde et al., 296 K (*18*)	92 ± 15	138 ± 11	91 ± 7	154 ± 6	147 ± 11
Δ%	13	−17	34	−14	−5
exp. Chattopadhyay et al. (*20*)				140	178
Δ%				−5	−22
exp. Tao and McMurry (*19*)			102.39	117.55	
Δ%			19.14	12.76	

[a] Δ% is the percentage deviation of the predicted value from the literature value.

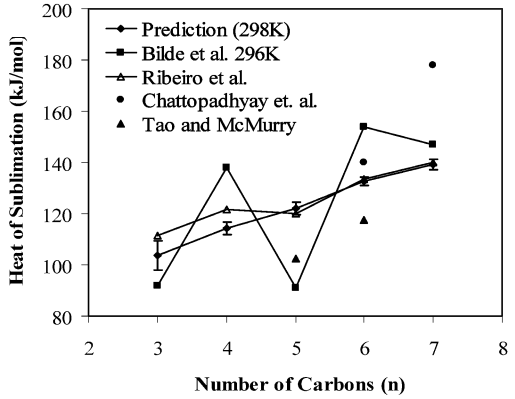

FIGURE 4. Comparison of calculated heats of sublimation for C_3-C_7 dicarboxylic acids against all available experimental data.

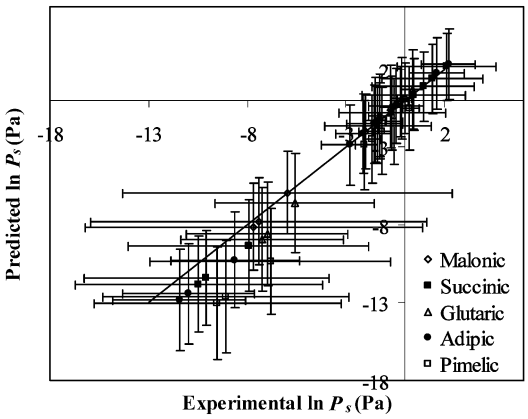

FIGURE 5. Predicted vs literature solid vapor pressure, ln P_s (in units of Pa) over the temperature range of ∼300 to ∼400 K for C_3-C_7 dicarboxylic acids. The solid line is the 1:1 correspondence line. Horizontal bars indicate the experimental uncertainty; vertical bars are 2σ from the predicted values. The upper group (ln P_s from ∼ −3 to 2) includes data from Riberio da Silva et al. (*22*) and leads to an average error of 21%. The lower group includes data from Bilde et al. (*18*) and leads to an average error of 70%.

from ∼1% to 10% (*25*, *33*), we estimated the error in the normal boiling points to be 10%. For melting points, values were obtained from the NIST Chemistry Webbook (*14*) (Tables 1 and 6), Experimental solid vapor pressure are usually determined from the Clausius−Clapeyron equation with the general form:

$$\ln P = -\frac{(\Delta H_{\mathrm{vap}} \pm \sigma_{\Delta H_{\mathrm{vap}}})}{RT} + (C \pm \sigma_{\mathrm{C}}) \qquad (6)$$

Uncertainties in experimental solid vapor pressures can be determined from $\sigma_{\Delta H_{\mathrm{vap}}}$ (see Table 5) and σ_{C} (*18*, *20*−*22*), The

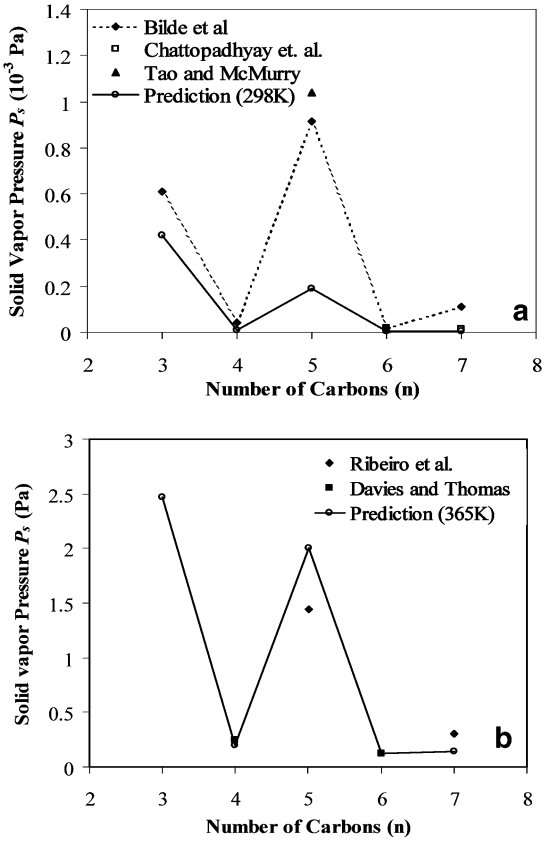

FIGURE 6. Odd−even effect. Comparison between predicted solid vapor pressures and various literature vapor pressure values for C_3-C_7 dicarboxylic acids at (a) 298 and (b) 365 K.

TABLE 6. Melting Points, Boiling Points, and Simulation Results for Formic, Acetic, and Benzoic Acids

	Formic	Acetic	Benzoic
Structure			
T_m (K)[a]	281.5 ± 0.6	289.6 ± 0.5	395.2 ± 0.7
T_b (K)[a]	373.9 ± 0.5	391.2 ± 0.6	523.2 ± 0.2
Target Temperature (K)	298.15	298.15	403.15
Target Density, ρ_0 (g/cm^3)	1.21	1.04	1.08
Simulation Density, ρ (g/cm^3)	1.09	1.04	1.08
Δ%	10.16	0.34	0.47
Calculated $\Delta H_{vap}(T_b)$ with ZPE correction (kJ/mol)	35.14 ± 2.6	39.70 ± 5.4	70.72 ± 5.2
$\Delta C_p(T_b)$ (J/mol K)	-75.22	-81.18	-108.14

[a] Values and uncertainties of the melting and boiling points are obtained from the NIST Chemistry webbook (*14*). Δ% is the percentage deviation of the predicted value from the literature value.

uncertainty of predicted ln(liquid/solid vapor pressure) generally decreases with increasing temperature, as shown in Figure 8.

TABLE 7. Predicted Liquid Vapor Pressures for Formic, Acetic, and Benzoic Acids[a]

temp (K)	exptl *P* (kPa)[b]	predicted *P* (kPa)	uncertainty in predicted *P* (kPa)	Δ%
		Formic Acid		
299.79	6.19	4.92	1.21	−20.50
307.58	8.88	7.42	1.65	−16.49
310.03	9.90	8.39	1.81	−15.19
316.8	13.29	11.66	2.31	−12.27
324.84	18.43	16.84	3.00	−8.62
329.03	21.83	20.21	3.41	−7.42
336.16	28.64	27.18	4.19	−5.09
344.58	38.85	37.78	5.27	−2.75
349.13	45.63	44.74	5.94	−1.96
353.36	52.45	52.07	6.63	−0.72
357.00	59.30	59.11	7.29	−0.31
364.87	76.34	76.84	8.98	0.65
			avg % error	−7.66
		Acetic Acid		
297.54	2.00	1.46	0.76	−27.24
304.76	3.00	2.28	1.07	−23.92
310.15	4.00	3.14	1.36	−21.50
318.14	6.00	4.91	1.87	−18.13
324.11	8.00	6.74	2.31	−15.77
328.92	10.00	8.60	2.70	−14.00
338.12	15.00	13.37	3.48	−10.84
355.32	30.00	28.20	4.74	−6.01
369.37	50.00	48.45	4.82	−3.09
374.69	60.00	58.64	4.41	−2.27
			avg % error	−14.28
		Benzoic Acid		
405.25	1.33	0.56	0.20	−57.81
419.85	2.67	1.32	0.39	−50.47
435.75	5.33	3.08	0.74	−42.23
445.95	8.00	5.09	1.06	−36.33
459.35	13.33	9.43	1.57	−29.24
478.95	26.66	21.43	2.38	−19.63
500.15	53.33	47.29	2.63	−11.32
522.35	101.32	98.74	0.64	−2.55
			avg % error	−31.20

[a] The uncertainties in the prediction and the percentage error were included. [b] Liquid vapor pressures obtained from DIPPR database (*13*).

The large uncertainty at low temperature may be due to the extrapolation of predicted heats of vaporization at 500 K to ambient temperature in addition to the linear dependence assumption in heats of vaporization. The relative error in the predicted vapor pressure (δP) can be calculated at different values of δV, where V can represent T_b, $\Delta H_{vap}(T_b)$, and $\Delta C_p(T_b)$; the perturbation (δV) is defined as

$$\delta V = \frac{V - V_{input}}{V_{max} - V_{input}} \quad (8)$$

The input values (V_{input}) are listed in Table 4 for the five dicarboxylic acids, and it is assumed that there can be a maximum variation of 10% in the input values. Table 7 shows the relative errors in predicted liquid pressure at 500 K for glutaric acid with different perturbations in T_b, $\Delta H_{vap}(T_b)$, and $\Delta C_p(T_b)$.

As shown in Table 8, the predicted liquid vapor pressure is most sensitive to normal boiling point (T_b) and least sensitive to the change in heat capacity $\Delta C_p(T_b)$. A 1% variation in boiling point changes δP from 0.67 to 0.40. The same variation in predicted heats of vaporization reduces δP to 0.63, and there is no change in δP with the 1% variation in $\Delta C_p(T_b)$. This order for glutaric (odd) acid also holds for adipic (even) acid, as shown in Figure 9. The normal boiling point is an important input parameter in the vapor pressure equation. Therefore, the vapor pressure method is usually applied to compounds with well-known normal boiling points. Nevertheless, we have shown that reasonable estimates for liquid vapor pressure can be obtained for dicarboxylic acids over a large temperature range even with an uncertainty of 10% in the input boiling temperatures.

The accuracy of the predicted heats of vaporization using CED directly depends on the accuracy of the force field used in the molecular simulations. To describe the strong hydrogen-bonding capability of dicarboxylic acids, we modified the hydrogen-bonding parameters in the Dreiding force field (*30*) to fit the QM results. We show that these new hydrogen-

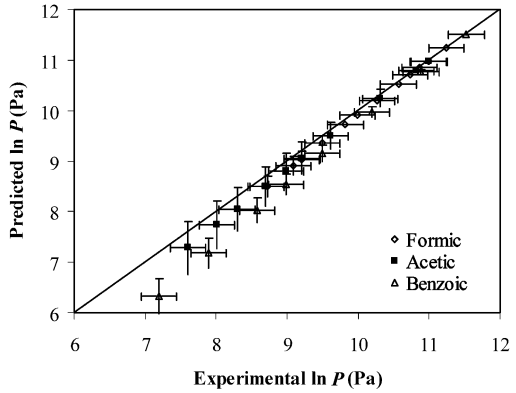

FIGURE 7. Predicted vs literature liquid vapor pressure, ln *P* (in the units of Pa) for formic, acetic, and benzoic acids. The solid line is the 1:1 correspondence line. The average error ranges from 8% (formic) to 31% (benzoic). Liquid vapor pressures obtained from DIPPR database (*13*).

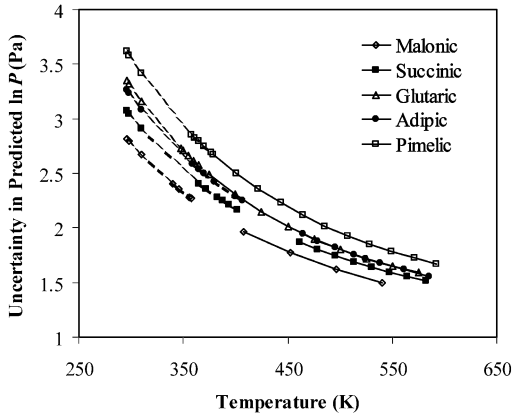

FIGURE 8. Uncertainties in solid vapor pressure (dotted line) and liquid vapor pressure (solid line), ln *P*, as a function of temperature for C_3−C_7 dicarboxylic acids

TABLE 8. Error in Predicted Liquid Vapor Pressure for Glutaric Acid at 500 K Relative to Experiment (DIPPR) (*13*)

parameter, *V*	range, V_{input} to V_{max}	perturbation, δV	relative error, δP
T_b	576−634 K	0	0.67
		0.1 (1%)	0.40
		0.5 (5%)	−0.30
		1 (10%)	−0.69
$\Delta H_{vap}(T_b)$	81.12−89.23 kJ/mol	0	0.67
		0.1 (1%)	0.63
		0.5 (5%)	0.48
		1 (10%)	0.31
$\Delta C_p(T_b)$	−112.64 to −123.90 J/molK	0	0.67
		0.1 (1%)	0.67
		0.5 (5%)	0.66
		1 (10%)	0.65

TABLE 9. Comparison between the Vapor Pressure (Pa) Predicted by Myrdal and Yalkowsky (*5*) Equation and Our Computational Chemistry Method at 500 K[a]

	malonic	succinic	glutaric	adipic	pimelic	avg % error
no. of carbons, *n*	3	4	5	6	7	
experimental[a]	7662.10	5211.60	4793.80	3257.00	2343.90	
our predictions	9254.29	5593.84	7904.17	2779.96	1813.53	26.1%
Myrdal and Yalkowsky (*5*) eq	4749.96	3137.96	5597.39	1434.64	1198.40	39.9%

[a] Experimental data were also included. [a] Liquid vapor pressure data obtained from DIPPR database (*13*).

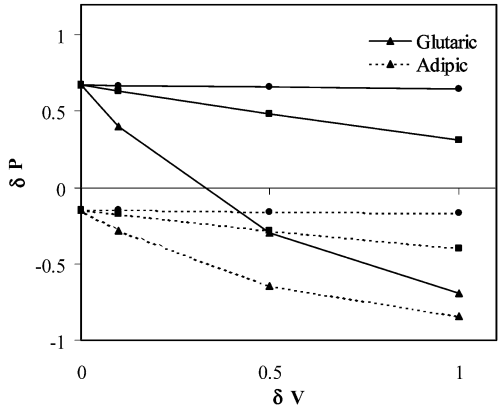

FIGURE 9. Sensitivity of the predicted liquid vapor pressure on the value of T_b (triangles), on the value of $\Delta H_{vap}(T_b)$ (squares), and on the value of $\Delta C_p(T_b)$ (circles) for glutaric acid at 500 K and adipic acid at 495 K.

bonding parameters are equally appropriate for other molecules containing the carboxylic acid functional group. In addition to mono- and dicarboxylic acids, the new hydrogen-bonding parameters are also applicable to aromatic monocarboxylic acids. For instance, we obtain an averaged error for predicted liquid vapor pressures of ~8% for formic acid, ~14% for acetic acid, and ~31% for benzoic acid, which is comparable to the overall average error of the C_3-C_7 diacids (~29%).

Little experimental data are available on the change of heat capacity upon boiling. Chickos et al. (*34*) calculated an average value of −134 J/mol K with a standard deviation of 71 J/mol K for most organic solids at 298 K. Their analysis also indicated that ΔC_p is not a strong function of temperature. The estimated $\Delta C_p(T_b)$ values using eq 4 (see Table 4) are well within the range of ΔC_p values observed by Chickos et al. (*34*). On the other hand, $\Delta C_p(T_b)$ can also be estimated by MD simulations, with results ranging from −139.08 J/mol K for succinic acid (C_4 diacid) to −315.26 J/mol K for pimelic acid (C_7 diacid). These values are outside the range of ΔC_p values observed by Chickos et al. (*34*). Using these MD predicted $\Delta C_p(T_b)$ values, a factor of 2 (or more) errors were found for the predicted liquid and solid vapor pressures. Therefore, we continue to use eq 4 for the input $\Delta C_p(T_b)$ values.

Myrdal and Yalkowsky (*5*) developed a vapor pressure estimation method that requires only the knowledge of transition temperatures and the molecular structure of the compound. Comparing their results to ours, we find (Table 8) that our predictive method performed better than the Myrdal and Yalkowsky equation (*5*) for liquid vapor pressures. For C_3-C_7 diacids, an average error of 40% was found for the Mydral and Yalkowsky equation (*5*), while the average error for our results is only 26%, as shown in Table 9.

Acknowledgments

This work was supported by National Science Foundation/Environmental Protection Agency Program TSE99-G No. 9985578 and the Electric Power Research Institute. We thank Dr. Shiang-Tai Lin and Rachel Niemer for their valuable discussions and suggestions. The facilities of the Materials and Process Simulation Center used in these calculations have been funded by DURIP-ONR, DURIP-ARO, NSF-MRI, and IBM (SUR Grant).

Appendix A: Determining the Hydrogen-Bonding Parameters in the Force Field

The accuracy of the molecular dynamics results directly depends on the accuracy of the force field. The hydrogen-bond parameters in the original Dreiding force field (*30*) were optimized for water dimers. However, these parameters do not account for the strong hydrogen-bonding ability of the carboxylic acid functional group.

To re-determine these parameters, we used density functional theory (DFT/B3LYP) QM calculations to calculate the interaction energies of the dimers, from which we extracted the hydrogen-bond parameters. The optimized hydrogen-bond parameters were used to compare molecular dynamics predictions of heats of vaporization, as explained in the paper, to experimental data without further optimization.

The Dreiding force field (*30*) uses the Lennard−Jones 12−10 function:

$$E_{hb}(r) = D_0\left[5\left(\frac{r_0}{r}\right)^{12} - 6\left(\frac{r_0}{r}\right)^{10}\right]\cos^4(\theta_{DHA})$$

to describe hydrogen-bonding interactions. Here r is the distance between the hydrogen-bond donor and acceptor, r_0 is the equilibrium hydrogen-bond distance between the donor and acceptor, and D_0 is the hydrogen-bond strength in kcal/mol. In addition, the energy depends on the angle θ_{DHA} between the bond of the H to the donor atom and the line between the donor and acceptor angle. The hydrogen-bond function in Dreiding uses $r_0 = 2.75$ Å and $D_0 = 4.00$ kcal/mol, parameters that were optimized for water dimers. These values are too large and too low, respectively, to represent the hydrogen bonding in dicarboxylic acids. For our acid systems, r would be the distance between the two oxygen atoms of the O···H−O hydrogen bond, as shown in Figure 10.

We assumed (and found) that formic and acetic acids form cyclic dimers with point group C_{2h} in the gas phase, as

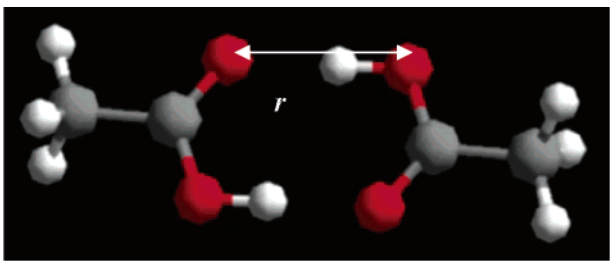

FIGURE 10. Dimeric configuration for acetic acid (C_{2h} symmetry).

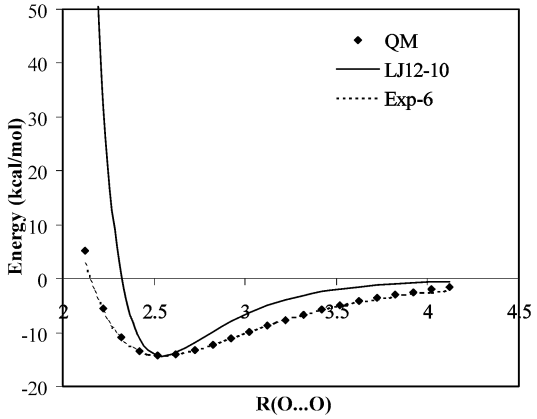

FIGURE 11. Comparison of QM results with fitted hydrogen-bonding energy curves for formic acid. The fitted functions are LJ12−10 and Exp-6.

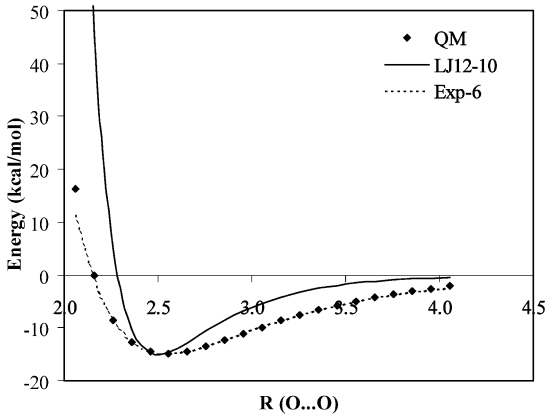

FIGURE 12. Hydrogen-bonding energy curve for acetic acid determined by both quantum mechanics and force field calculation and the fitted LJ12−10 and Exp-6 functions.

established previously with experiment and computation (*35*, *36*). To determine the appropriate parameters for organic acids:

(i) The binding energy curve of the acid dimer, as a function of the *r*, was obtained from QM (DFT/B3LYP).

(ii) Using Mulliken charges at optimum geometries of the monomer derived from the DFT/B3LYP method, we calculated the similar binding energy curve using the Dreiding force field, but the hydrogen-bonding function was turned off.

(iii) The difference between the two binding energy curves was taken as the hydrogen-bonding energy curve.

(iv) Optimum values for D_0 and r_0 were determined by fitting the above function to the hydrogen-bonding energy curve.

For formic acid, the LJ12−10 hydrogen-bonding function fits well with the calculated hydrogen-bonding energy curve with $r_0 = 2.55$ Å and $D_0 = 7.15$ kcal/mol (Figure 11). Other functional forms could be used to describe hydrogen bonding. For instance, we find that an exponential-6 (Exp-6) function:

$$E_{hb}(r) = D_0\left\{\left(\frac{6}{\zeta - 6}\right)\exp\left[\zeta\left(1 - \frac{r}{r_0}\right)\right] - \left(\frac{\zeta}{\zeta - 6}\right)\left(\frac{r_0}{r}\right)^6\right\}$$

fits the hydrogen-bonding energy for a wider range of hydrogen-bond donor−acceptor distance (R(O···O)) with $r_0 = 2.55$ Å, $D_0 = 7.15$ kcal/mol, and $\zeta = 9.37$. However, the default LJ12−10 function seems sufficiently accurate for our systems.

The hydrogen-bonding parameters were also determined for acetic acid in a similar fashion. For acetic acid, the r_0 and D_0 are found to be 2.50 Å and 7.50 kcal/mol, respectively, for LJ12−10. The Exp-6 potential fits well for the same r_0 and D_0 values with $\zeta = 9.34$. (see Figure 12). The total binding energy curve as a function of *r* was also determined for acetic acid with the LJ12−10 hydrogen-bonding potential. Figure 13 shows that the binding energy from force field calculation with the new parameters ($r_0 = 2.50$ Å and $D_0 = 7.50$ kcal/mol) agrees well with the QM calculations.

We determined new hydrogen-bonding parameters for carboxylic acid functional groups based on the formic and acetic acid dimer results. For dicarboxylic acid systems, the hydrogen-bond parameters determined using acetic acids should be more appropriate than those determined by formic acids. Chao and Zwolinski (*35*) determined the enthalpy of dimerization for acetic acid to be 15.10 kcal/mol. Our calculated value using the new hydrogen-bonding parameters is 14.96 kcal/mol. Thus, we have shown that ab initio determined hydrogen-bond parameters can provide reasonable estimates for the binding energy, heats of vaporization, and vapor pressures of the carboxylic acids presented here.

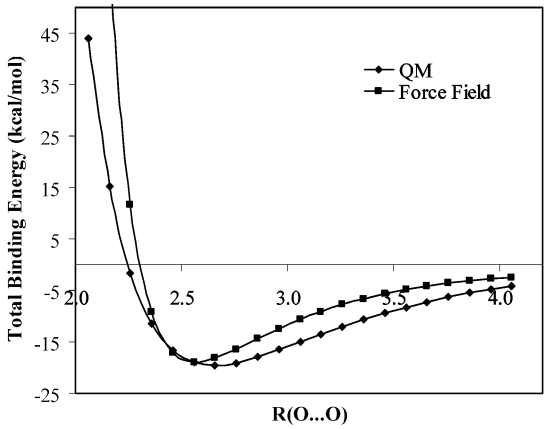

FIGURE 13. Total binding energy curves for the acetic acid dimer determined using QM and force field calculations with new hydrogen-bonding parameters. Negative energies are binding; positive energies are repulsive.

Literature Cited

(1) Pankow, J. F. An absorption model of gas/particle partitioning of organic compounds in the atmosphere. *Atmos. Environ.* **1994**, *28*, 185−188.

(2) Pankow, J. F. An absorption model of the gas/aerosol partitioning involved in the formation of secondary organic aerosol. *Atmos. Environ.* **1994**, *28*, 189−193.

(3) Pankow, J. F.; Seinfeld, J. H.; Asher, W. E.; Erdakos, G. B. Modeling the formation of secondary organic aerosol. 1. Application of theoretical principles to measurements obtained in the α-pinene, *β*-pinene, sabinene, Δ^3-carene, and cyclohexene−ozone systems. *Environ. Sci. Technol.* **2001**, *35*, 1164−1172.

(4) Seinfeld, J. H.; Asher, W. E.; Erdakos, G. B.; Pankow, J. F. Modeling the formation of secondary organic aerosol (SOA). 2. The predicted effects of relative humidity on aerosol formation in the α-pinene, *β*-pinene, sabinene, Δ^3-carene, and cyclohexene−ozone systems. *Environ. Sci. Technol.* **2001**, *35*, 1806−181.

(5) Myrdal, P. B.; Yalkowsky, S. H. Estimating pure component vapor pressures of complex organic molecules. *Ind. Eng. Chem. Res.* **1997**, *36*, 2494−2499.

(6) Asher, W. E.; Pankow, J. F.; Erdakos G. B.; Seinfeld J. H. Estimating the vapor pressures of multi-functional oxygen-containing organic compounds using group contribution methods. *Atmos. Environ.* **2002**, *36*, 1483−1498.

(7) Saxena, P.; Hildemann, L. M. Water-soluble organics in atmospheric particle—a critical review of the literature and application of thermodynamics to identify candidate compounds. *J. Atmos. Chem.* **1996**, *24*, 57−109.

(8) Kawamura, K.; Steinberg, S.; Kaplan, I. R. Concentrations of monocarboxylic and dicarboxylic acids and aldehydes in

southern California wet precipitations: Comparison of urban and non-urban samples and compositional changes during scavenging. *Atmos. Environ* **1996**, *30* (7), 1035−1052.
(9) Kawamura, K.; Kasukabe, H.; Barrie, L. A. Source and reaction pathways of dicarboxylic acids, ketoacids and dicarbonyls in arctic aerosols: One year of observations. *Atmos. Environ* **1996**, *30* (10−11), 1709−1722.
(10) Kawamura, K.; Sakaguchi, F. Molecular distributions of water soluble dicarboxylic acids in marine aerosols over the Pacific Ocean including tropics, *J. Geophys. Res.* [*Atmos.*] **1999**, *104* (D3), 3501−3509.
(11) Narukawa, M.; Kawamura, K.; Takeuchi, N.; Nakajima, T. Distribution of dicarboxylic acids and carbon isotopic compositions in aerosols from 1997 Indonesian forest fires. *Geophys. Res. Lett*. **1999**, *26* (20), 3101−3104.
(12) Prenni, A. J.; Demott, P. J.; Kreidenweis, S. M.; Sherman, D. E. The effects of low molecular weight dicarboxylic acids on cloud formation. *J. Phys. Chem. A* **2001**, *105*, 11240−11248.
(13) Daubert, T. E.; Danner, R. P. *Physical and Thermodynamic Properties of Pure Chemicals: Data Compilation*; Hemisphere: New York, 1994.
(14) Afeefy, H. Y.; Liebman, J. F.; Stein S. E. Neutral thermochemical data. In *NIST Chemistry WebBook, NIST Standard Reference Database Number 69*; Linstrom, P. J., Mallard, W. G., Eds.; National Institute of Standards and Technology: Gaithersburg, MD, March 2003 (http://webbook.nist.gov).
(15) Thodos, G.; Forman, J. C. Critical temperature and pressures of organic compounds. *AICHE J.* **1960**, *6*, 206.
(16) Lide, D. R. *CRC Handbook of Chemistry and Physics*, 79th ed.; CRC Press: Boca Raton, FL, 1998.
(17) Stull, D. R. Vapor pressure of pure substances. *Ind. Eng. Chem*. **1947**, *39*, 517.
(18) Bilde, M.; Svenningsson, B.; Mønster, J.; Rosenørn, T. Even−odd alternation of evaporation rates and vapor pressures of C_3−C_9 dicarboxylic acid aerosols. *Environ. Sci. Technol*. **2003**, *37*, 1371−1378.
(19) Tao, Y.; McMurry, P. H. Vapor pressures and surface free energies of C_{14}−C_{18} monocarboxylic acids and C_5 and C_6 dicarboxylic acids. *Environ. Sci. Technol*. **1989**, *23*, 1519−1523.
(20) Chattopadhyay, S.; Tobias, H. J.; Ziemann, P. J. A method for measuring vapor pressures of low-volatility organic aerosol compounds using a thermal desorption particle beam mass spectrometer. *Anal. Chem*. **2001**, *73*, 3797−3803.
(21) Davies, M.; Thomas, G. H. The lattice energies, infra-red spectra, and possible cyclization of some dicarboxylic acids. *Trans. Faraday Soc.* **1960**, *56*, 185−192.
(22) Ribeiro da Silva, M. A. V.; Monte, M. J. S.; Ribeiro, J. R. Vapor pressures and the enthalpies and entropies of sublimation of five dicarboxylic acids. *J. Chem. Thermodyn*. **1999**, *31*, 1093−1107.
(23) Thalladi, V. R.; Nüsse, M.; Boses, R. The melting point alternation in α,ω-alkanedicarboxylic acids. *J. Am. Chem. Soc.* **2000**, *122*, 9227−9236.
(24) Voutsas, E.; Lampadariou, M.; Magoulas, K.; Tassios, D. Prediction of vapor pressures of pure compounds from knowledge of the normal boiling point temperature. *Fluid Phase Equilib*. **2002**, *198*, 81−93.
(25) Baum, E. J. *Chemical Property Estimation*: *Theory and Application*; CRC Press: Boca Raton, FL, 1998.
(26) Belmares, M.; Blanco, M.; Ross, R. B.; Caldwell, G.; Chou, S.-H.; Pham, J.; Olofson, P. M.; Goddard, W. A., III. Hildebrand and Hansen solubility parameters from molecular dynamics with applications to electronic nose polymer sensors. *Environ. Sci. Technol*. in press.
(27) Becke, A. D. Density-functional thermochemistry III. The role of exact exchange. *J. Chem Phys*. **1993**, *98* (7), 5648−5652.
(28) Xu, X.; Goddard, W. A., III. Bonding properties of water dimer: A comparative study of density functional theories. *J. Comput. Chem*. (in press).
(29) Brameld, K.; Dasgupta, S.; Goddard, W. A., III. Distance dependent hydrogen bond potentials for nucleic acid base pairs from ab initio quantum mechanical calculations (LMP2/cc-pVTZ). *J. Phys. Chem. B* **1997**, *101* (24), 4851−4859.
(30) Mayo, S. L.; Olafson, B. D.; Goddard, W. A., III. Dreiding: A generic force field for molecular simulations. *J. Phys. Chem*. **1990**, *94*, 8897−8909.
(31) Riedel, L. Eine neue universelle damfdruck-formal (A new universal vapor pressure equation). *Chem. Ing. Tech*. **1954**, *26*, 83.
(32) Vapor pressures and critical points of liquids. XVII. Aliphatic carboxylic acids and anhydrides; Item 80029; Engineering Sciences Data: London, 1980.
(33) Boethling, R. S.; Mackay, D. *Handbook of property estimation methods for chemicals: environmental and health sciences*; Lewis: Boca Raton, FL, 2000.
(34) Chickos, J. S.; Hesse, D. G.; Liebman, J. F. A group additivity approach for the estimation of heat capacities of organic liquids and solids. *Struct. Chem*. **1993**, *4*, 271−277.
(35) Chao, J.; Zwolinski, B. J. Ideal gas thermodynamic properties of methanoic and ethanoic acids. *J. Phys. Chem. Ref. Data* **1978**, *7* (1), 363−377.
(36) Minary, P.; Jedlovszky, P.; Mezei, M.; Turi, L. A comprehensive liquid simulation study of neat cormic acid. *J. Phys. Chem. B* **2000**, *104*, 8287−8294.

Received for review December 18, 2003. Revised manuscript received April 26, 2004. Accepted May 4, 2004.

ES0354216